

Dopamine Induces Apoptosis through an Oxidation-involved SAPK/JNK Activation Pathway*

(Received for publication, September 3, 1997, and in revised form, October 16, 1997)

Yongquan Luo^{‡§}, Hiroyuki Umegaki[‡], Xiantao Wang[‡], Ryoichi Abe[‡], and George S. Roth[‡]

From the [‡]Molecular Physiology and Genetics Section and the [§]Gene Expression and Aging Section, Gerontology Research Center, NIA, National Institutes of Health, Baltimore, Maryland 21224

Dopamine (DA) is a neurotransmitter, but it also exerts a neurotoxic effect under certain pathological conditions, including age-related neurodegeneration such as Parkinson's disease. By using both the 293 cell line and primary neonatal rat postmitotic striatal neuron cultures, we show here that DA induces apoptosis in a time- and concentration-dependent manner. Concomitant with the apoptosis, DA activates the JNK pathway, including increases in JNK activity, phosphorylation of c-Jun, and subsequent increase in c-Jun protein. This DA-induced JNK activation precedes apoptosis and is persistently sustained during the process of apoptosis. Transient expression of a dominant negative mutant SEK1(Lys → Arg), an upstream kinase of JNK, prevents both DA-induced JNK activation and apoptosis. A dominant negative c-Jun mutant FLAGΔ169 also reduces DA-induced apoptotic cell death. Anti-oxidants *N*-acetylcysteine and catalase, which serve as scavengers of reactive oxygen species generated by metabolic DA oxidation, effectively block DA-induced JNK activation and subsequent apoptosis. Thus, our data suggest that DA triggers an apoptotic death program through an oxidative stress-involved JNK activation signaling pathway. Given the fact that the anti-oxidative defense system declines during aging, this molecular event may be implicated in the age-related striatal neuronal cell loss and age-related dopaminergic neurodegenerative disorders, such as Parkinson's and Huntington's diseases.

Dopamine (DA)¹ is a neurotransmitter under physiological conditions. However, accumulating evidence indicates that DA may also serve as a neurotoxin and thereby participates in the neurodegenerative process. This includes ischemia (1), local exposure to high concentrations of excitatory amino acids (2), and treatment with methamphetamine (3, 4). The DA availability in animal striatum is significantly increased in the above cases. In the case of hypoxia, the striatal DA levels are increased by up to 1100% of control levels (5). Direct injection

of high concentration of DA (0.025–0.5 M) into the striatal area results in neurodegeneration (6). DA, 6-OH-DA, and other monoamines are also neurotoxic when directly applied to cell cultures (7–9).

The mechanism of DA neurotoxicity is highly linked to oxidative metabolism. With respect to its molecular structure, DA contains an unstable catechol moiety. DA can oxidize spontaneously *in vitro* or through an enzyme-catalyzed reaction *in vivo* to form reactive oxygen species (ROS), free radicals, and quinones (10–12). In the human substantia nigra, the DA oxidation products may further polymerize to form another neurotoxin, neuromelanin (13). These oxidation products can damage cellular components such as lipids, proteins, and DNA (14). Although the cause of age-related degeneration of dopaminergic neurons in Parkinson's disease (PD) is unknown, the oxidative stress induced by DA is believed a major pathological factor. In the "free radical hypothesis," the neurodegeneration in PD is considered to result from high exposure of these dopaminergic neurons to ROS, especially generated by oxidation of DA (15, 16). This hypothesis is supported by postmortem studies showing that in the substantia nigra of PD brain, there are increased indices of oxidative stress, increased levels of iron, increased lipid peroxidation, decreased mitochondrial complex I activity, and decreased levels of glutathione (GSH) (17, 18). Indeed, *in vitro* studies show that DA (0.01–1 mM) and its metabolic product, 6-OH-DA, can induce apoptosis associated with ROS in a variety of cell types. These include both neuronal and non-neuronal cells, for example primary neonatal rat striatal cell cultures (19, 20), primary chick sympathetic neurons (8), a cloned catecholaminergic cell line (CATH.a) derived from the central nervous system (21), human neuroblastoma NMB cells (22), neuronal PC12 cells (23), and even mouse thymocytes (24). Application of anti-oxidants, such as *N*-acetylcysteine, catalase, ascorbic acid, and dithiothreitol (DTT) can effectively prevent DA-induced apoptotic cell death (8, 19, 21, 24). However, the molecular events involved in the processes of DA-induced apoptosis are unknown.

Recent evidence suggests that the JNK (also called SAPK) pathway may play an important role in triggering apoptosis in response to free radicals generated by ultraviolet and gamma radiation, or direct application of H₂O₂, or inflammatory cytokines (tumor necrosis factor α , interleukin-1) (25–29). In response to the above cellular stresses, JNK is strongly activated (26, 27). Overexpression of dominant negative mutants of components in the JNK pathway, such as ASK1(K709R), SEK1(Lys → Arg) (both are upstream kinases), and c-Jun Δ169 (a downstream target), can effectively prevent the apoptosis (29–32). Furthermore, transfection of the constitutively activated forms of ASK1, SEK1, or c-Jun results in apoptotic cell death (29–32). Given the role of the JNK pathway in initiating apoptosis, we test here the hypothesis that DA-induced apoptosis may also be mediated by JNK activation. We have used both 293 cells and

* The costs of publication of this article were defrayed in part by the payment of page charges. This article must therefore be hereby marked "advertisement" in accordance with 18 U.S.C. Section 1734 solely to indicate this fact.

§ To whom correspondence should be addressed: Molecular Physiology and Genetics Section, Gerontology Research Center, NIA, National Institutes of Health, 4E02, 4940 Eastern Ave., Baltimore, MD 21224. Tel.: 410-558-8507; Fax: 410-558-8323; E-mail: luoyq@helix.nih.gov.

¹ The abbreviations used are: DA, dopamine; ERK, extracellular signal-regulated kinase; GST, glutathione S-transferase; JNK, c-Jun N-terminal kinase (also called SAPK); MAPK, mitogen-activated protein kinase; MOPS, 4-morpholinopropanesulfonic acid; NGF, nerve growth factor; PAGE, polyacrylamide gel electrophoresis; SEK1, SAPK/Erk kinase 1; DTT, dithiothreitol; PBS, phosphate-buffered saline; IMEM, improved minimum essential medium (Eagle's with 4 mM glutamine; ROS, reactive oxygen species; PD, Parkinson's disease; DAPI, 4,6-diamidino-2-phenylindole; NAC, *N*-acetylcysteine.

primary neonatal rat striatal cell cultures to test this hypothesis. Our results indicate that DA indeed triggers cellular apoptosis through an oxidation-linked JNK activation pathway.

EXPERIMENTAL PROCEDURES

Materials—Antibodies against JNK-1 and GST were from Santa Cruz Biotechnology. Monoclonal anti-c-Jun was from Oncogene. Antibodies against phospho-specific c-Jun (Ser-63) II and phospho-specific SAPK/JNK were from New England Biolabs. Anti-Flag M2 monoclonal antibody was from Kodak. Dopamine was from Research Biochemicals. A dominant negative SEK1(Lys → Arg) vector was provided by Dr. L. Zon and J. Kyriakis; pCDFLAG169 DNA was from Dr. L. Rubin and J. Ham.

Cell Cultures and Treatments—The 293 cells were maintained in IMEM supplemented with 10% fetal bovine serum with 100 units/ml penicillin and 100 µg/ml streptomycin. For primary neonatal striatal cell cultures, the procedures were described previously (33). The striata of neonatal rats (Wistar rat colony of Gerontology Research Center, NIA, National Institutes of Health) were dissected and pooled in Hank's balanced salt solution at 4 °C. Cells were enzymatically dispersed by a mixture of 0.15% collagenase and 0.001% DNase. The cells were then plated on polyethyleneimine-coated chamber slides and cultured in a medium (50% Dulbecco's modified Eagle's medium, 50% Ham's F-12) supplemented with 5% fetal bovine serum and 5% horse serum at 37 °C with 5% CO₂. After 3 days, 5 µM cytosine arabinofuranoside was included to inhibit growth of glial cells and fibroblasts. Cell culture medium was routinely changed every 3 to 4 days. Cells were used after 20 days in culture to perform experiments.

To determine changes in JNK activity, phosphorylation of c-Jun and c-Jun protein levels in 293 cells, we incubated the cells with DA in 1% serum-containing medium to reduce background. Apoptosis was determined under the same conditions. In striatal cell cultures, the cells were treated with DA in the complete medium.

DNA Analysis and Detection of Apoptotic Cells—The procedure for extraction of DNA was followed as described (23). 1×10^8 293 cells were used to isolate DNA for each sample. Cells were harvested by gentle scraping and collected by centrifugation for 5 min at 4 °C. The pellet was resuspended with TE buffer (5 mM Tris-HCl, pH 8.0; 20 mM EDTA) containing 0.5% v/v Triton X-100 for 20 min at 4 °C. To remove high molecular weight DNA, the samples were centrifuged at 14,000 rpm for 30 min in the presence of 0.1% SDS. The samples were then sequentially extracted with equal volumes of a mixture of phenol:chloroform:isoamyl alcohol (25:24:1) and chloroform. The DNA was precipitated with 0.1 volume of 5 M NaCl and 2 volumes of ethanol at -70 °C overnight. The DNA was resuspended with TE buffer, and the RNA was digested by 0.1 mg/ml RNase for 3 h at 30 °C. The samples were run on 1.4% agarose gels containing 0.1 µg/ml ethidium bromide, and DNA was visualized under UV light.

For detection of apoptotic cells, the cells were first washed twice with cold PBS and then fixed with 4% paraformaldehyde for 30 min. The fixed cells were washed again with PBS and stained with 1 µg/ml 4,6-diamidino-2-phenylindole (DAPI) solution for 30 min. The apoptotic cells were examined under a fluorescence microscope. Cells containing condensed or fragmented nuclei were scored as apoptotic. Data are expressed as percentage of apoptotic cells in total counted cells.

Transient Expressions—Lipofectin® reagent was used to transfect cDNA plasmids by following the protocol provided by manufacturer (Life Technologies, Inc.). After transfection, the cells were fed with complete medium for 1 additional day. These cells were then used for experiments.

Lysate Preparation—For determination of JNK activity and anti-JNK1 immunoblotting, cell extracts were prepared as follows. Stimulated cells were scraped into tubes and collected by centrifugation at 4000 rpm for 5 min at 4 °C. The cell pellets were washed with cold PBS and solubilized with ice-cold JNK lysis buffer consisting of 25 mM Hepes, pH 7.5, 300 mM NaCl, 1.5 mM MgCl₂, 0.2 mM EDTA, 0.1% Triton X-100, 20 mM β-glycerophosphate, 0.1 mM sodium orthovanadate, 0.5 mM DTT, 100 µg/ml phenylmethylsulfonyl fluoride, and 2 µg/ml leupeptin. The cellular extract was then centrifuged for 30 min at 14,000 rpm to remove debris. The supernatant was used immediately or aliquoted and stored at -70 °C for further use. For anti-phospho-specific c-Jun and c-Jun immunoblotting, we have used different procedures. Stimulated cells were collected as described above. The cell pellets were washed with cold PBS, solubilized with hot SDS lysis buffer (80–90 °C) consisting of 10 mM Tris-HCl (pH 7.6), 150 mM NaCl, 0.5 mM EDTA, 1 mM EGTA, 1% SDS, 1 mM sodium orthovanadate, and a mixture of protease inhibitors (1 mM phenylmethylsulfonyl fluoride, 1 µg/ml pep-

statin A, 2 µg/ml aprotinin) and heated for 10 min at 90 °C. The lysates were then sonicated for 10 s and centrifuged for 20 min in a microcentrifuge. The supernatants were used to perform SDS-PAGE or stored at -70 °C.

Measurement of JNK Activity—The procedures described by Coso *et al.* (34) were used with a slight modification. Clarified cell lysates (200 µg of proteins) were first incubated overnight at 4 °C with 10 µg of polyclonal anti-JNK1 and then incubated with 20 µl of Sepharose A-conjugated protein A for an additional 1 h. The beads were pelleted and washed three times with cold PBS containing 1% Nonidet P-40 and 2 mM sodium orthovanadate, once with cold 100 mM Tris-HCl (pH 7.5) buffer containing 0.5 M LiCl, and once with cold kinase reaction buffer consisting of 12.5 mM MOPS (pH 7.5), 12.5 mM β-glycerophosphate, 7.5 mM MgCl₂, 0.5 mM EGTA, 0.5 mM NaF, and 0.5 mM sodium orthovanadate. The kinase reaction was performed in the presence of 1 µCi of [γ -³²P]ATP, 20 µM ATP, 3.3 µM DTT, and 3 µg of substrate GST-c-Jun (1–98) in kinase reaction buffer for 30 min at 30 °C and stopped by addition of 10 µl of 5 × Laemmli loading buffer. The samples were heated for 5 min at 95 °C and analyzed by 12% SDS-PAGE. Phosphorylated substrate c-Jun was visualized by autoradiography. The optical density of autoradiograms was determined using the NIH Image program. The kinase activity was expressed as fold of control.

Western Immunoblotting and Immunocytochemistry—Equal amounts of lysate protein (40 µg/lane) were run on either 10 or 8–16% SDS-PAGE and electrophoretically transferred to nitrocellulose. Nitrocellulose blots were first blocked with 10% nonfat dry milk in TBST buffer (20 mM Tris-HCl (pH 7.4), 500 mM NaCl, and 0.01% Tween 20) and then incubated with primary antibodies (JNK-1, 1:1000, Santa Cruz Biotechnology; Ser(P)-73-specific c-Jun and phospho-SAPK/JNK, 1:1000, New England Biolabs; monoclonal c-Jun, 1:1000, Oncogene; monoclonal anti-Flag M2, 1:1000, Kodak) in TBST containing 5% bovine serum albumin overnight at 4 °C. Immunoreactivity was detected by sequential incubation of horseradish peroxidase-conjugated secondary antibody (1:5000, Jackson ImmunoResearch) and Renaissance substrate (DuPont). For immunocytochemical studies, cells were first washed twice with cold PBS and then fixed with 4% paraformaldehyde in PBS. Immunostaining was performed according to the procedures provided by the manufacturer for the ABC Elite kit. Nonspecific binding was blocked with 5% normal goat or horse serum for 1 h in TBST buffer (50 mM Tris-HCl (pH 7.4), 150 mM NaCl, 0.1% Triton X-100) for 1 h. The cells were then incubated with primary antibody (polyclonal anti-D2 receptor, 1:1000, Chemicon; monoclonal anti-Flag M2, 1:1000, Kodak) overnight at 4 °C in a TBST solution. They were sequentially incubated for 1 h with biotinylated secondary antibody, ABC reagents for 1 h, and then exposed for 5 min to a mixture of hydrogen peroxide, and chromogen, 3,3'-diaminobenzidine tetrahydrochloride. The positive staining cells were examined under a light microscope.

Protein Determination—Two methods were used depending on the detergents used in the preparation of cell lysates. The protein concentration in cellular extracts containing Triton X-100 was determined by Bio-Rad protein reagent (Bio-Rad), and protein in the lysates containing SDS was measured by MicroBCA kit (Pierce product).

RESULTS

Dopamine Induces Apoptosis in Non-neuronal and Neuronal Cell Cultures—We have chosen human embryo kidney 293 cells and neonatal striatal cell cultures as non-neuronal and neuronal cells, respectively, to study the apoptotic effect of dopamine. One of the biochemical features of apoptosis is the early onset of specific endonuclease cleavage of cellular DNA into a nucleosome ladder (35). Considering the limited amount of material available from neonatal rat striatal cell cultures, we first used 293 cells to find optimal conditions for DA-induced apoptosis by examining DNA fragmentation (DNA ladder). 293 cells were plated on 60-mm dishes and grown to about 80% confluency. The cells were then exposed to DA in IMEM containing 1% serum. As expected, DA induced a typical apoptotic DNA ladder with a 200-base pair range increase (Fig. 1, A and B). DA induced DNA fragments in a time- and concentration-dependent manner (Fig. 1, A and B). Exposure of 293 cells to 500 µM DA resulted in DNA cleavage beginning at 16 h and reaching a maximum at 30 h (Fig. 1A). Within 30 h of exposure, DA induced DNA fragmentation at concentrations from 100 µM to at least 500 µM (Fig. 1B). We have repeated these experiments at least 3 times and observed similar time- and concentration-dependent patterns. DA-induced nuclear changes were evalu-

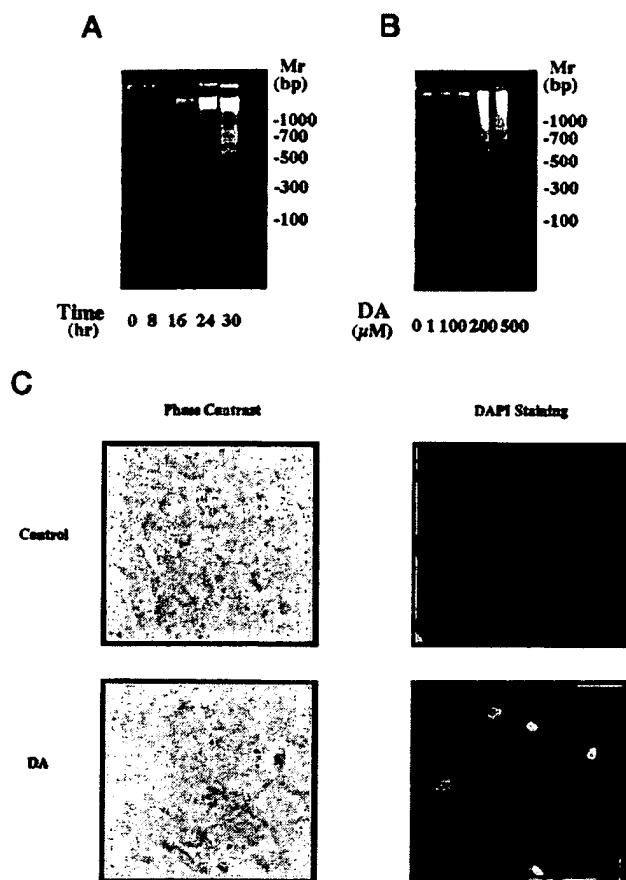


FIG. 1. DA induces apoptosis in 293 cells. *A*, time course of DA-induced DNA fragmentation. 293 cells were plated on 60-mm dishes and were cultured to about 80% confluency. The cells were then exposed to 500 μ M DA in 1% serum containing IMEM for different times. Soluble cytoplasmic DNA was isolated and run on 1.4% agarose gels. The DNA was stained with ethidium bromide. *B*, concentration-dependent DNA ladder induced by DA. 293 cells were exposed to different concentrations of DA in a 1% serum-containing IMEM for 30 h. Cytoplasmic DNA fragments were isolated using the same method as in *A*. The last lane in *A* and *B* shows a DNA marker indicated on the right side of the both panels. *C*, morphological profiles of DA-induced apoptosis. Neonatal rat striatal cells, after 20 days culture, were treated with 500 μ M DA or vehicle (Control) for 24 h, fixed, and stained with DAPI. The left panel shows phase contrast pictures; the right panel shows DAPI staining fluorescence. The arrows in left panel indicate typical apoptotic cells with round shape corresponding to chromatin condensation in the right panel. All pictures were taken 40 \times magnification.

ated under a fluorescence microscope using DAPI staining. In control cells, the nuclei showed uniform staining, indicating that cells were healthy and nuclei were intact. With 500 μ M DA treatment for 30 h, some nuclei exhibited typical apoptotic characteristics, such as nuclear condensation and fragmentation (not shown). Apoptotic cells represented $70 \pm 5.3\%$ ($n = 4$) of those cells. Some floating dead cells were also observed at this time point. Based on these observations, we chose maximal stimulation with 500 μ M DA for 30 h to observe the DA apoptotic effect in neonatal rat striatal cell cultures.

Neonatal rat striatal cells were prepared and cultured for 20 days. To identify striatal cell cultures, we examined expressions of D₂-dopamine receptor protein and mRNA, respectively. For receptor protein, we immunostained the cell cultures with anti-D2R antibody. As expected, the cultures showed positive anti-D2R staining of 40–60% of cells. The D2R was mostly located on the cell surface. These cells were not stained by the same dilution of normal rabbit serum (data not shown). Receptor mRNA levels were detected by reverse transcription-

polymerase chain reaction as described (36, 37). As expected, these cells expressed both D2RL and D2RS isoforms (data not shown). In agreement with previous report of autoradiography by ³H-labeled ligand receptor binding (33), the neonatal rat striatal cell cultures contain D2R expressing neurons. These cells were used to observe apoptotic effects of DA. DA (500 μ M) was added for 24 h, and the cells were then fixed with 4% paraformaldehyde in PBS. Under a light microscope, the apoptotic cells appeared round and shrunken (indicated by arrows in the lower left panel of Fig. 1C). Corresponding to these changes, the nuclei appeared typically condensed and fragmented by DAPI staining (lower right panel, Fig. 1C). Some cells also underwent early apoptosis as indicated by strong chromatin fluorescence although they appeared similar in cell size (lower right panel, Fig. 1C). The apoptotic cells represented about $31 \pm 4.6\%$ ($n = 5$) of the total population. Thus, our results suggest that DA induces apoptosis in both non-neuronal and neuronal cells.

DA Activates the JNK Pathway—Activation of the JNK pathway has been implicated in initiating apoptosis in several cases. These include deprivation of NGF from sympathetic neurons and NGF-differentiated PC12 cells (30, 32) and exposure of the cells to lethal dosages of γ and UV-c irradiation (25, 38). To test the hypothesis that DA-induced apoptosis may involve the JNK pathway, we examined the effects of DA on this pathway, which include JNK activation, phosphorylation of c-Jun, and the amount of c-Jun in both 293 cells and neonatal rat striatal cell cultures.

We first characterized the JNK assay using 293 cells (Fig. 2). The kinase activity was linear with reaction times between 0 to 30 min and remained steady from 30 to 60 min. The kinase activity was also linear with the cell protein concentration between 0 and 200 μ g and saturated between 200 and 500 μ g of protein. Based on these results, we used 200 μ g of cell lysate protein and 30-min reaction times for further experiments.

DA stimulated the JNK pathway in a time- and concentration-dependent manner. In the presence of 1% serum, 293 cells were stimulated by application of 500 μ M DA for various times. Cellular lysates were prepared and JNK activity determined with anti-JNK1 immunocomplex kinase assay. DA induced JNK activity up to 9.3-fold compared with controls when the cells were stimulated for 3 h (Fig. 3A). This DA-stimulated JNK activation was sustained for at least 27 h in our time course studies (from 3 to 30 h, Fig. 3A). The JNK activation was accompanied by a small increase (10–20%) in JNK1 protein determined by Western immunoreactivity with anti-JNK1 from time 0 to 30 h (Fig. 3A). This small increase in JNK1 immunoreactivity may be due to reduced migration of phosphorylated JNK1 enzyme. Following the activation of JNK1, phosphorylation of c-Jun, a target of JNK1, was also increased during DA stimulation. The phosphorylated c-Jun was detected using anti-specific phospho-c-Jun (Fig. 3A). Corresponding to the time course of JNK1 activation by DA, phosphorylation of c-Jun began at 3 h and reached a maximum at 23 h. DA also increased the amount of c-Jun with a similar time course to phosphorylation of c-Jun. At 30 h, all activation of the JNK pathway including JNK activity, phosphorylation of c-Jun, and synthesis of c-Jun was decreased. This may be due to apoptotic cell death at this time point as was shown in Fig. 1A. We have also examined the concentration effect of DA on the JNK pathway. 293 cells were exposed to different concentrations of DA from 1 to 500 μ M in the presence of 1% serum. For determination of JNK activation, the cells were stimulated with DA for 3 h. For detection of c-Jun protein, the cells were exposed to DA for 23 h. DA stimulated the JNK pathway in a dose-dependent manner (Fig. 3B). This activation of the JNK pathway by DA is

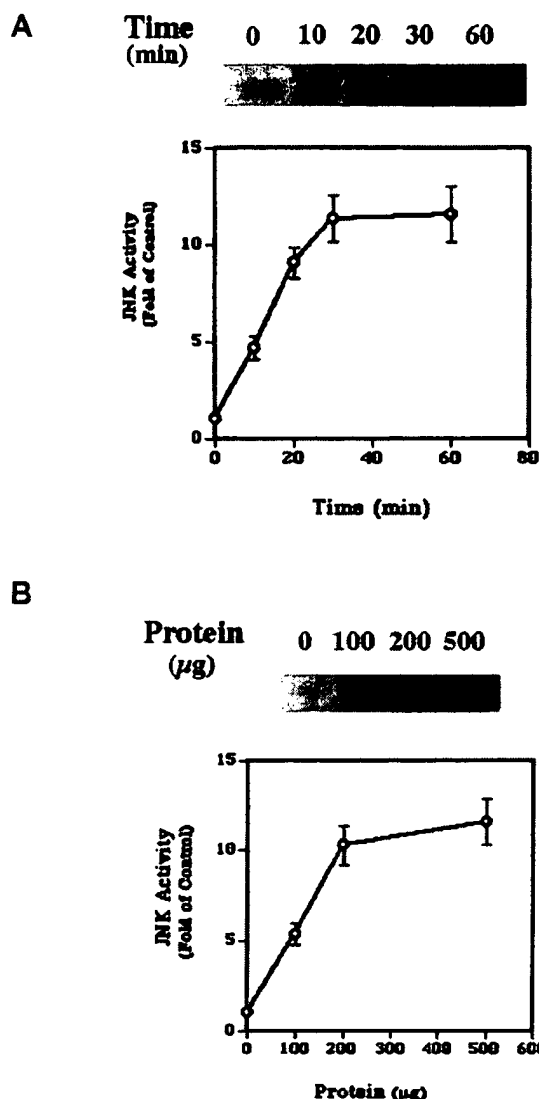


FIG. 2. Characterization of the JNK assay. 293 cells were stimulated with 500 μ M DA for 3 h. The cell lysates were prepared and immunoprecipitated with 10 μ g of polyclonal anti-JNK1 followed by 20 μ l of Sepharose A-conjugated protein A. The kinase reaction was performed by the procedures described under "Experimental Procedures." **A**, time course of the kinase reaction. The top represents the autoradiogram of [γ - 32 P]ATP incorporation into exogenous GST-c-Jun-(1-98). The amount of cell lysate used was 200 μ g of protein in each lane. The bottom figure is a plot of JNK activity versus time. The values in this figure are means (\pm S.E.) of three determinations. **B**, protein concentration effect. Anti-JNK1 immunocomplexes were obtained with various amounts of the cell lysates as indicated. The JNK assay was performed for 30 min as described under "Experimental Procedures." The top is a representative autoradiogram. The bottom shows quantified data from three determinations (means \pm S.E.). The control is the value determined at 0 protein concentration.

detectable at 100 μ M and increased with elevated concentrations (Fig. 3B). This dose-response activation of the JNK pathway was shown by a 32 P incorporation kinase assay and increase of anti-c-Jun immunoreactive protein (Fig. 3B). DA had little or no effect on the amount of JNK1 protein determined by anti-JNK1 immunoreactivity (Fig. 3B).

DA also stimulated the JNK pathway in neonatal rat striatal cell cultures. A paradigm of DA stimulation similar to that for 293 cells was used except that the striatal cell cultures were maintained in complete culture medium. Like the pattern for 293 cells, 500 μ M DA increased JNK activity about 6-fold after 4 h (Fig. 3C). This concentration of DA also increased the

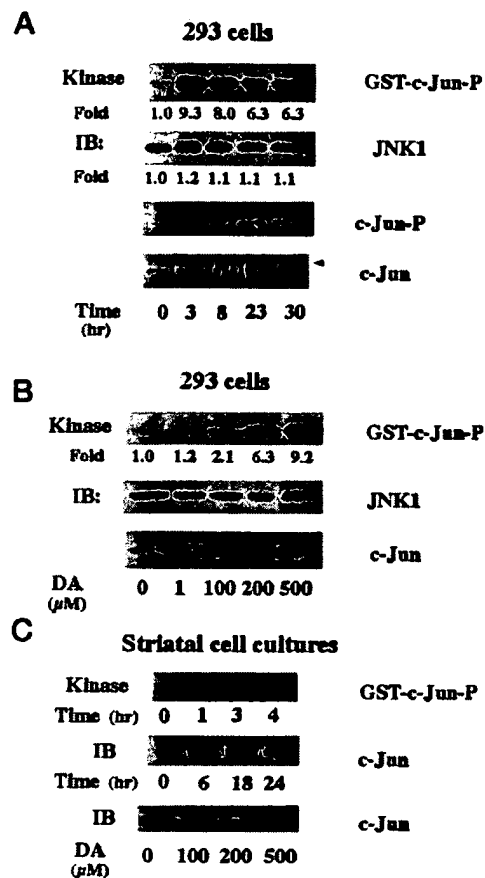


FIG. 3. DA activates the JNK pathway. **A**, time course of activation of the JNK pathway by DA. 293 cells were stimulated with 500 μ M DA for different times. JNK activity was determined using an anti-JNK1 immunocomplex kinase assay and exogenous GST-c-Jun-(1-89) as a substrate. The protein of JNK1, phosphorylated c-Jun, and c-Jun were determined using Western immunoblotting (IB) with corresponding antibodies. The JNK activity and anti-JNK1 immunoreactivity were quantified using the NIH Image 1.55 program and expressed as a fold of control (0 time) under each band. **B**, concentration-dependent effects of DA on the JNK pathway. The procedures for kinase assay and Western immunoblotting were identical to those in **A**. JNK activation and the JNK1 immunoblotting with increasing concentrations were measured from the samples exposed to DA for 3 h. c-Jun was determined using samples treated with DA for 23 h. **C**, effects of DA on the JNK pathway in neonatal striatal cell cultures. For time course studies, the striatal cell cultures were challenged with 500 μ M DA. For dose-response, the cells were exposed to DA for 18 h. The kinase activity determination and immunoblotting procedures are the same as in **B**.

anti-c-Jun immunoreactive band at 6 h and peaked at 18 h (Fig. 3C). Following exposure of the cell culture to different concentrations of DA from 100 to 500 μ M for 18 h, amounts of c-Jun protein were also correspondingly increased (Fig. 3C).

By comparing the kinetics of JNK activation (Fig. 3) with that of apoptosis (Fig. 1) by DA, it is evident that stimulation of the JNK pathway occurs before apoptotic cell death. In both 293 cells and striatal cell cultures, activation of JNK appeared after 3 to 4 h exposure to 500 μ M DA. Apoptotic cell death occurred after 16 h. Moreover, the dose dependence of the JNK pathway activation by DA is parallel to its ability to induce cell death. These results suggest that the JNK pathway may be involved in triggering the apoptosis by DA.

JNK/SAPK Signaling Mediates DA-induced Apoptosis—As mentioned earlier, the JNK/SAPK pathway involves an orderly activation of proteins, MEKK1, SEK1, JNK, and c-Jun (26, 27, 31). SEK1 is an upstream kinase of JNK, and c-Jun is a downstream substrate of activated JNK. We assessed roles of the

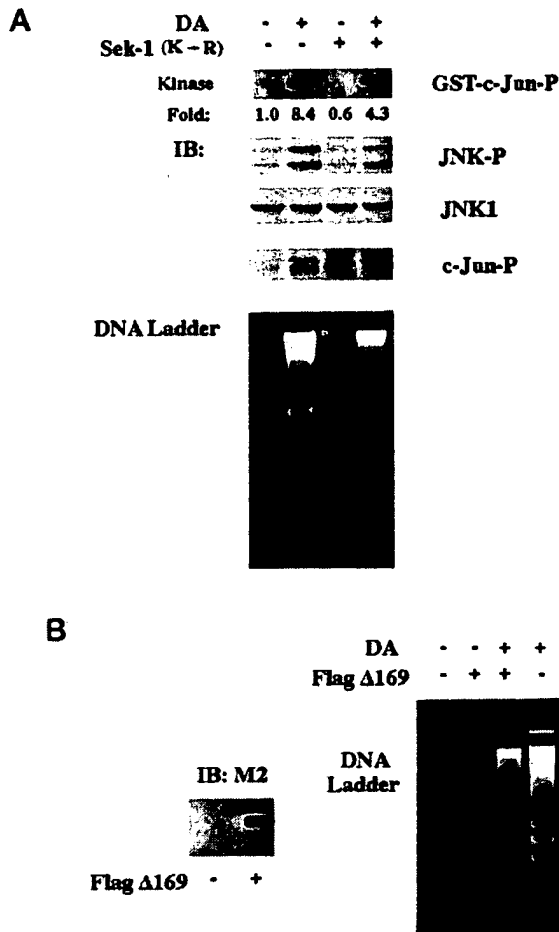


FIG. 4. Block of JNK pathway inhibits DA-induced apoptosis in 293 cells. **A**, a negative mutant SEK1(Lys → Arg) inhibits activation of the JNK pathway and apoptosis induced by DA. 293 cells were plated on 60-mm dishes and transfected with a total of 2 μ g/ml DNA of either empty vector (–) or mutated SEK1 (+). After 2 days, the cells were incubated with 500 μ M DA (+) or vehicle (–) for 8 h. The cellular lysates were prepared. The JNK activity and immunoblottings were determined as described. Antibody against phospho-specific JNK can recognize both phosphorylated JNK1 (46 kDa, lower band) and phosphorylated JNK2 (54 kDa, higher band). For DNA ladder, the cells were treated with DA for 30 h. The picture shows that transfection of a dominant negative SEK1 mutant significantly inhibited JNK activation and apoptosis by DA. **B**, dominant negative c-Jun mutant FlagΔ169 reduces DA-induced apoptosis. *Left panel*, immunoblotting of transfected FlagΔ169 (+, 2 μ g/ml DNA) or its empty vector (–, 2 μ g/ml) of 293 cells with monoclonal anti-Flag (M2, 1:1000). *Right panel*, DNA ladder analysis due to 500 μ M DA (30 h) under conditions of either transfected FlagΔ169 (+, 2 μ g/ml) or its empty vector (–, 2 μ g/ml).

JNK pathway in DA-induced apoptosis using a dominant negative SEK1(Lys → Arg) mutant and a c-Jun negative mutant FlagΔ169.

pEBG-SEK1(Lys → Arg) is a dominant negative kinase-inactive construct (29). In U937 cells, its transfection efficiency is about 39% (29). Expression of SEK1(Lys → Arg) in U937 cells inhibits C₂-ceramide or H₂O₂-induced endogenous JNK activity by 50% and completely inhibits the co-transfected hemagglutinin-tagged JNK (29). By using 293 cells, we have transiently transfected this SEK1 negative mutant that is tagged by GST. Its expression was detected by anti-GST immunoblotting (data not shown). By co-transfection with pCMV β carrying β -galactosidase gene and staining with 5-bromo-4-chloro-3-indolyl β -D-galactopyranoside, we calculated that the transfection efficiency was about 30–50% in 293 cells. Overexpression of this SEK1(Lys → Arg) mutant inhibited DA (500 μ M for

TABLE I
A dominant negative SEK1(Lys → Arg) inhibits DA-induced apoptosis

293 cells were transfected either with SEK1(Lys → Arg) (2 μ g/ml) or its empty vector for 2 days. The cells were then treated with 500 μ M DA or left untreated (control) for 24 h. Apoptotic cells were examined with DAPI staining under a fluorescence microscope. Data are presented as means (\pm S.E., $n = 3$) of the percentage of apoptotic cells in all cells indicated in parentheses.

Groups	Control	DA
Empty vector	4.5 \pm 1.3 (4450)	68.6 \pm 6.3 (4240)
SEK1(Lys → Arg)	5.3 \pm 1.4 (4360)	30.5 \pm 5.4 (4725)

3 h)-induced endogenous JNK activity by 49 \pm 6.7% ($n = 4$) compared with the control group (Fig. 4A). Accordingly, transiently transfected SEK1(Lys → Arg) also inhibited phosphorylation of JNK1 detected by specific anti-phospho-JNK antibody (Fig. 4A). This phospho-specific antibody can recognize both phospho-JNK1 (46 kDa, a lower band) and phospho-JNK2 (54 kDa, a higher band, Fig. 4A). Furthermore, the transfection of SEK1 mutant also significantly inhibited phosphorylation of c-Jun, consequently resulting in reduction of DA-induced apoptosis indicated by either DNA ladder (500 μ M DA for 30 h; Fig. 4A) or DAPI staining (500 μ M DA for 24 h, Table I). However, the transfection of SEK1 mutant did not affect JNK1 expression (Fig. 4A). Thus, these observations suggest that SEK1-JNK1-c-Jun activation is involved in DA-induced apoptosis.

Next, we examined the effects of a dominant negative c-Jun mutant, FLAGΔ169, on DA-induced apoptosis. This mutant was generated from the mouse c-Jun cDNA by deleting sequences that encode the NH₂-terminal c-Jun transactivation domain (amino acids 1–168) (32, 39). This c-Jun Δ169 lacks the ability to activate transcription but is still capable of dimerization and binds to DNA (40). The c-Jun Δ169 vector is tagged by an 8-amino acid FLAG epitope in place of NH₂-terminal Δ169, allowing monitoring of its expression by Western immunoblotting or immunocytochemistry with monoclonal anti-M2 (32). We transiently transfected 293 cells with this c-Jun Δ169, and its expression was detected by anti-M2 immunoblotting (Fig. 4B). Its transfection efficiency was about 30–50% as determined by both anti-M2 immunocytochemistry and co-transfection with pCMV β vector expressing β -galactosidase. After 2 days transfection, the cells were exposed to 500 μ M DA for 30 h. Cytoplasmic DNA was prepared and visualized using ethidium bromide staining. Compared with empty vector transfected 293 cells (lane 4, right panel, Fig. 4B), c-Jun Δ169 effectively reduced DA-induced DNA fragmentation (lane 3, right panel, Fig. 4B). The transfection of c-Jun Δ169 itself did not affect cell behavior since no DNA ladder was observed (lane 2, Fig. 4B). Supporting the data from the above negative SEK1 mutant experiments, DA induces apoptosis through a SEK1, JNK1, and c-Jun pathway.

More and more evidence indicates that c-Jun is a killer protein in developing neurons. Overexpression of activated c-Jun produces apoptosis, and suppression of c-Jun protects against neuronal death induced by deprivation of NGF in sympathetic neurons (32, 41) and neonatal hippocampal neurons (42). Based on the above non-neuronal data and increase of c-Jun expression by activation of the JNK pathway in neonatal striatal cells (Fig. 3C), we assumed that activation of c-Jun might play a key role in DA-induced apoptosis in striatal cells. To test this, we transfected c-Jun Δ169 in neonatal rat striatal cells after 20 days in culture. The transfection was carried out in the presence of both 5 μ g/ml insulin and 1% serum for 8–12 h. The expression of Δ169 was confirmed by anti-M2 immuno-

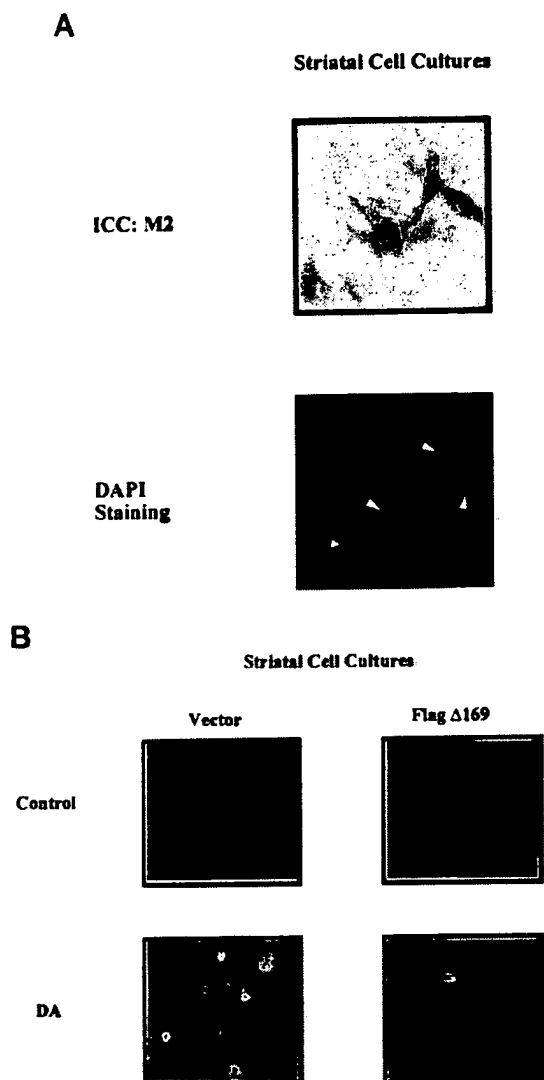


FIG. 5. A dominant negative c-Jun mutant prevents DA-induced apoptosis in striatal cell cultures. A, anti-Flag immunocytochemistry and profile of DA-induced apoptosis. Neonatal striatal cells, cultured for 20 days, were transfected either with 2 μ g/ml Flag Δ 169 or its empty vector. After 2 more days in culture, the cells were treated with either 500 μ M DA or left untreated for 24 h. The cells were fixed and immunostained with monoclonal anti-Flag M2. After immunocytochemistry, the cells were stained with DAPI. The picture shows the same field of M2 immunocytochemistry and DAPI staining of Flag Δ 169-transfected cells with DA treatment. The arrows indicate the cells corresponding to the M2-positive cells. B, morphological effect of Flag Δ 169 on DA-induced apoptosis. The procedures for transfection and treatment were the same as in A. After that, the cells were stained by DAPI, and the pictures (40 \times magnification) were taken under a fluorescence microscope. Vector, empty vector.

cytochemistry (top panel, Fig. 5A), and the transfection efficiency was about 20–40%. Under these conditions, we did not observe obvious Lipofectin toxicity. Following treatment with 500 μ M DA for 24 h, we did not observe apoptosis in the anti-M2 positive staining cells (lower panel, Fig. 5A, the cells indicated by arrows correspond to the anti-M2 positive cells at the top), although there were some adjacent cells showing apoptotic chromatin condensation. We repeated this experiment at least three times and observed similar results. However, there was a weak DAPI fluorescence staining in positive anti-M2 cells although they showed normal morphological characteristics under a light microscope. This weak DAPI staining may result from interference with the brown color of the immunocyto-

TABLE II
A dominant negative c-Jun Flag Δ 169 inhibits DA-induced apoptosis

Groups	Control	DA
Empty vector	7.2 \pm 1.8 (1065)	33.6 \pm 3.2 (1245)
Flag Δ 169	7.3 \pm 1.0 (2136)	11.5 \pm 2.0 (2688)

Neonatal striatal cells were transfected either with Flag Δ 169 (2 μ g/ml) or its empty vector for 2 days. After that, the cells were treated with 500 μ M DA for 24 h. Apoptotic cells were examined with DAPI staining and counted under a fluorescence microscope. Data are expressed as means (\pm S.E., $n = 5$) of the percentage of apoptotic cells in all cells indicated in parentheses.

chemistry and affected our quantitation of the data. To avoid this problem, we directly determined apoptotic cells using DAPI staining compared with the empty vector transfected group without anti-M2 immunocytochemistry. The morphological changes and percentage of apoptotic cells are shown in Fig. 5B and Table II, respectively. In the empty vector control group, treatment with DA (500 μ M) significantly increased apoptotic cells (34 \pm 3%; $n = 5$) indicated by chromatin condensation and DNA fragmentation. The transfected Δ 169 group showed significant inhibition of apoptosis by DA (12 \pm 2%; $n = 5$). Both the empty vector and the Δ 169 groups show only a low background cell death. Thus, inhibition of c-Jun activation prevents apoptosis induced by DA.

Anti-oxidants Protect against DA-induced Apoptosis by Inhibition of JNK Activation—Although DA-induced apoptosis may involve multiple mechanisms, recent evidence suggests that oxidative stress may play an essential role (8, 19, 21, 24). Due to the inherent instability of the catechol moiety of DA, the molecule readily oxidizes to form reactive oxygen species, free radicals, and quinones through autooxidation or enzyme-catalyzed reactions (10–12). These free radicals may initiate apoptosis, since anti-oxidants, such as catalase and *N*-acetylcysteine (NAC), can block DA-induced apoptosis in different types of cells (8, 19, 21, 24). Given that the DA-induced apoptotic cell death is mediated by the JNK pathway, we examined the effects of anti-oxidants on DA-induced JNK activation and subsequent apoptosis.

Anti-oxidants NAC and catalase inhibited both DA-induced JNK activity and apoptosis. 293 cells were plated on 60-mm dishes and cultured to 80% confluency. The cells were first treated with NAC (1 mM) or catalase (10,000 units/ml) or left untreated (control) for 30 min. These cells were then exposed to 500 μ M DA for either 3 or 30 h for determining JNK activity and apoptotic cell death, respectively. As indicated in Fig. 6A, DA alone significantly increased JNK activity and resulted in apoptotic DNA fragmentation. Preincubation of NAC and catalase completely blocked JNK activation and cell death (Fig. 6A). NAC and catalase alone did not have any effect on JNK activity and cell morphological changes. By using a similar protocol, we also tested these compounds on DA-induced apoptotic cell death in neonatal rat striatal cells after 20 days in culture. Similar results were obtained to those for 293 cells (see Fig. 6, B and C). Thus, anti-oxidants protect against DA-induced cell death through inhibition of JNK activation, providing another piece of evidence for an essential role of JNK activation in DA-induced apoptosis.

DISCUSSION

In this paper, we present evidence that DA induces apoptosis in both the 293 cell line and postmitotic striatal neuronal cell cultures. The characteristic apoptotic changes are similar to those observed in other cell types, including cell shrinkage, loss

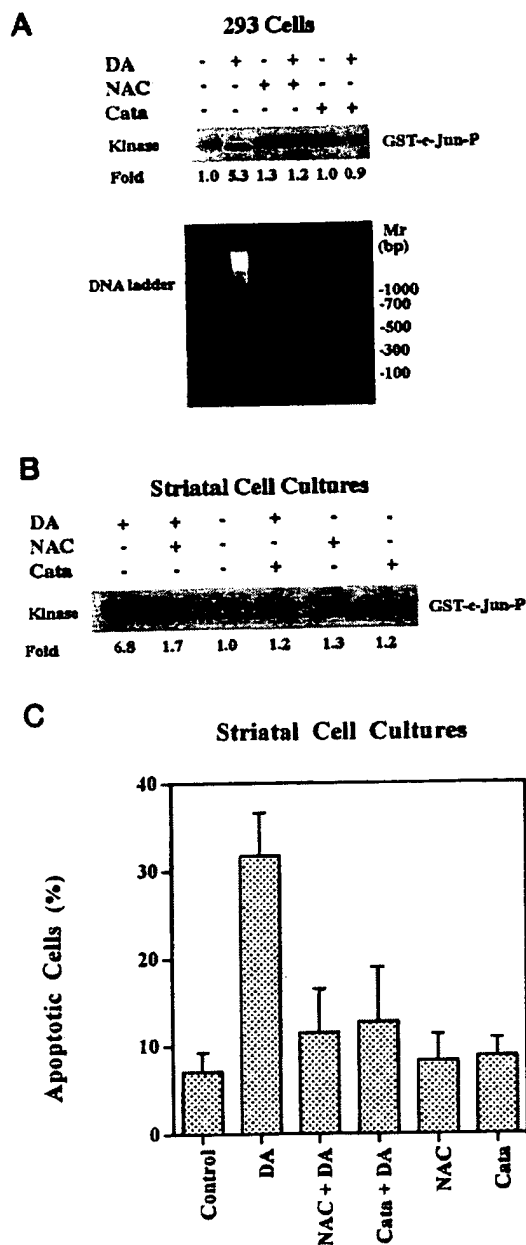


FIG. 6. Anti-oxidants inhibit both DA-induced JNK activity and apoptosis. **A**, 293 cells. 293 cells were plated on 60-mm dishes and cultured to 80% confluency. The cells were first treated with 1 mM NAC (+) or 10,000 units of catalase (+) or without treatment (-) for 0.5 h and then challenged with 500 μ M DA (+) or vehicle (-). For kinase assays, the cells were stimulated with DA for 3 h (top panel). For DNA ladder analysis, the cells were exposed to DA for 30 h (bottom panel). **B** and **C**, neonatal rat striatal cells. The procedures for treatment of cells with anti-oxidants and DA were the same as those in **A**. Neonatal striatal cells were used after 20 days in culture and treated first with either anti-oxidants NAC (1 mM) and catalase (Cata; 10,000 units/ml) or vehicle for 0.5 h. The cells were then exposed to DA for 4 and 24 h to determine JNK activity (**B**) and apoptosis, respectively. Apoptotic cells were counted with a fluorescence microscope after DAPI staining. Data represent mean (\pm S.E.) of percentage of apoptotic cells from three independent experiments (**C**).

of contact with neighboring cells, nuclear condensation, and fragmentation. We also provided evidence suggesting that the DA-induced apoptosis is mediated by DA oxidation linked to the JNK activation pathway. First, exposure of the cells to DA activates the JNK pathway, including phosphorylation and activation of JNK enzyme, phosphorylation of c-Jun, and in-

crease of c-Jun protein. Second, the DA stimulation of the JNK pathway precedes apoptotic processes. The JNK activation increases after 3–4 h of treatment with DA, whereas apoptotic cells appear after 16 h exposure of the cells to DA. The DA-induced JNK activation pathway tightly correlates with the subsequent apoptosis in a concentration-dependent manner. Third, and most importantly, a dominant negative SEK1 mutant can block DA-induced JNK activation and subsequent phosphorylation of c-Jun as well as apoptosis. Consistent with this result, a negative c-Jun mutant, which presumably blocks c-Jun activation, also inhibits apoptotic cell death by DA. Finally, anti-oxidants, such as NAC and catalase, which both serve as scavengers of free radicals generated by oxidation of DA, completely prevent activation of the JNK and consequent apoptosis. Thus, our data suggest a model by which DA produces ROS, then activates the JNK pathway, resulting in triggering of apoptosis.

Our results indicate that DA induces a persistent activation of the JNK enzyme, which may play a critical role in initiating the apoptotic suicide program. DA strongly stimulates JNK activity after 3 to 4 h exposure of cells and maintains it before and during apoptosis for at least 27 h (Fig. 3A). This longer and sustained JNK activation may serve as a death signal in DA-induced apoptosis. In agreement with this view, a similar longer stimulation of the JNK enzyme was also observed in some environmental stress-induced forms of apoptosis. For example, exposure of Jurkat cells to lethal doses of γ and UV-c radiation rapidly increases JNK activity after 30 min and can last at least 12 h without significant effect on p38 MAP kinase and ERK activity (25, 38). Withdrawal of NGF from differentiated PC12 neuronal cells results in persistent activation of JNK and p38 MAP kinase with inhibition of ERK activity (30). Although there are variable effects on p38 MAP kinase and ERK activities in the different cell systems described above, the JNK activation is persistent and shows a direct correlation with the apoptosis. Furthermore, repression of JNK activation by transfection of a dominant negative mutant JNK1 prevents γ and UV-c irradiation-induced apoptosis (25, 38). Overexpression of a dominant negative mutant of upstream kinase MEKK1 for JNK inhibits apoptosis induced by deprivation of NGF from differentiated PC12 cells (30). In our case, transfection of a dominant negative mutant of SEK, an upstream kinase for JNK, also blocks DA-induced apoptosis (Fig. 4A and Table I). All of these observations indicate that a longer and sustained JNK activation is essential to induce apoptosis in some types of cell death. The DA-induced persistent JNK activation may be produced by the continued stimulation of upstream enzymes of JNK due to cellular damage by ROS of DA oxidation (see below). The alternative pathway for prolonged JNK activation may be inactivation of dual specificity phosphatase, an enzyme that can dephosphorylate JNK and ERK resulting in down-regulation of the activities (43).

DA treatment also results in sustained activation of c-Jun protein. c-Jun is a transcription factor and can positively autoregulate its own expression by JNK which can directly bind to and phosphorylate the c-Jun transactivation domain on serines 63 and 73 (27, 44). DA increases both the amount of c-Jun and the phosphorylation of c-Jun with a similar time course. This observation suggests that the phosphorylated c-Jun could be entirely due to the increase in c-Jun protein. The increased c-Jun protein could be phosphorylated since JNK enzyme was still highly activated during this time (Fig. 3A). Our data are also similar to the observation by Ham *et al.* (32) that NGF withdrawal results in an increase in c-Jun protein accompanied by slower migration of phosphorylated c-Jun. This positive feedback regulatory mechanism for c-Jun activation may play a

crucial role in triggering apoptosis induced by DA.

It should also be noted that the time course of JNK activation differs from that of c-Jun phosphorylation. One possible explanation might be a difference in the time required for active JNK to translocate from the cytosol to the nucleus. Another possibility might be the existence of a c-Jun phosphatase whose activation is affected by dopamine.

How does activation of the JNK pathway by DA induce apoptosis? One possibility is that activation of JNK pathway may stimulate the genes that promote cell proliferation. Like the hypothesis of apoptosis of sympathetic neurons induced by withdrawal of neurotrophic factors, cell death is assumed to result from an inappropriate attempt to reenter the cell cycle in such terminally differentiated neurons (32, 45, 46). According to this model, deprivation of neurotrophic factor would trigger expression of genes related to cyclin-dependent kinases that promote entry into the cell cycle. By using a reverse transcription-polymerase chain reaction technique, Freeman *et al.* (47) reported that cyclin D1 mRNA is selectively increased at 15–20 h after NGF withdrawal. During this time, the sympathetic neuron is subject to dying. Ham *et al.* (32) suggested that cyclin D1 expression is probably driven by c-Jun-involved AP-1 activity since the cyclin D1 promoter has a potential AP-1 binding site and c-Jun is activated 4–8 h after NGF deprivation. Consistent with this model, there was a report that DA can alter cell cycle and force human neuroblastoma NMB cells to accumulate in S/M₂ phase (22). This alteration of the cell cycle by DA accompanies apoptosis, peaking at 16–24 h, and is concentration-dependent. Cycloheximide, a protein synthesis inhibitor, blocks both changes in the cell cycle and apoptosis induced by DA (22). In agreement with this view, our results show that the JNK pathway is stimulated after DA application for 3 h. It might be expected that c-Jun activation through the DA-induced JNK pathway stimulates AP-1 activity-involved cell cycle gene transcription that promotes cell proliferation. NAC, in addition to its anti-oxidation effect, also inhibits cell proliferation in PC12 cells (48). The ability of NAC to inhibit DNA synthesis is parallel to its function to promote survival of PC12 cells and sympathetic neurons following deprivation of serum or NGF (48). Our data show that NAC also inhibits both DA-induced JNK activation and apoptosis. It is possible that DA stimulates the JNK pathway and then activates cell cycle gene expression through c-Jun-dependent AP-1 activity, driving cells into an inappropriate cell cycle, such as accumulation in the S/G₂ phase, finally resulting in apoptosis. NAC, a scavenger of free radicals generated by DA, inhibits JNK activity and potential subsequent abortive attempts to re-enter the cell cycle, thus preventing cell death. Although the current data favor this model, other possibilities still exist. For example, DA-induced JNK activity may regulate interleukin-1 β converting enzyme family members.

The oxidative products of DA may serve as stimuli to activate the JNK pathway and subsequent apoptosis. As mentioned in the Introduction, DA can be metabolized to form ROS, such as H₂O₂, O₂⁻, and OH⁻ through either autooxidation or enzyme-catalyzed reactions (10–12). Like other environmental stresses, such as ionizing irradiation, UV radiation, and heat shock, the ROS can activate both JNK and apoptosis in a variety of cell systems (29). In agreement with this idea, our data show that anti-oxidants including NAC, a scavenger of ROS, and catalase, an enzyme that hydrolyzes H₂O₂ into H₂O and O₂, prevent DA-induced JNK activation and subsequent apoptosis. Other anti-oxidants, such as ascorbic acid and DTT, also have protective effects against DA toxicity (8, 20). Bcl-2 is an oncogene product and is intracellularly located in the places where ROS is generated, such as mitochondria, endoplasmic

reticulum, and nuclear membranes (49). Bcl-2 inhibits ROS-induced apoptosis through regulation of an anti-oxidation pathway (49). Using an antisense probe on Bcl-2 to reduce its expression increases the sensitivity of the CATH.a cell line to the toxic effects of DA (21). Moreover, overexpression of Bcl-2 in PC12 cells can block JNK activity induced by deprivation of serum (50). *In vivo*, since the enzymes catalyzing DA metabolism occur intracellularly, blockage of the DA transporter by either application of its selective inhibitors, such as bupropion, or down-regulation using antisense oligonucleotides effectively reduces DA cytotoxicity in bovine chromaffin cells and human neuroblastoma NMB cells, respectively (22, 51). Blockage of DA entry into these cells is assumed to reduce the generation of ROS. We are currently investigating the potential mechanisms of ROS production by DA activation of the JNK pathway and apoptosis.

The molecular events of DA oxidation-JNK pathway may be implicated in senescent DA receptor containing neuron loss in striatum. One of the most obvious manifestations of brain aging is a selective loss of D₂-dopamine receptors from the corpus striatum (52). This decrement has been observed in rodents, as well as primates including humans (52, 53). During aging, D₂-dopamine (DA) receptor-containing neurons in striatum are decreased about 25–30% (52, 54). Although the cause of the neuron death is not well understood, recent evidence suggest that apoptosis may be involved in this process. In old rats, the frequency of apoptotic striatal cells is significantly increased compared with young animals (55). In aged rodent brains, decreased levels of GSH and mitochondrial cytochromes as well as mitochondrial dysfunction have been reported (56, 57). Anti-oxidant activities are also reported to be decreased during aging (58). These senescent changes would accumulate ROS products of DA, resulting in activation of an apoptotic suicide program.

It is known that apoptosis is a normal process during development. In certain brain regions, cell death can occur in 50% of the neurons produced by neurogenesis (59). From this view, apoptosis is considered an active process to protect the organism from mutation and overgrowing (60). During development of dopaminergic neurons, DA has been shown to be required for neurogenesis (61). As cell proliferation and apoptosis often share similar biochemical pathways, increased levels or enhanced overflow of DA due to hypoxia or exposure to excitatory amino acids may trigger apoptosis of postmitotic neurons in the brain, based on our *in vitro* data. However, in the case of Parkinson's disease, the anti-oxidative system including catalase, glutathione peroxidase, as well as levels of glutathione are decreased in substantia nigra neurons, suggesting greater susceptibility to the oxidative stress produced by DA (15, 16). Recent *in vitro* data show that the levels of GSH are important to maintain the granular storage of DA in rat PC12 cells (62) and function of DA transport in the rat striatal synaptosomes (63). The normal catecholamine concentration in dopaminergic cell bodies is estimated to be approximately 0.1–1 mM (64). Based on the above information, one may hypothesize why the selective increase of DA oxidation exists in the age-related PD brain. Indeed, in substantia nigra, the increased oxidation of DA is observed by an increased ratio of free cysteinyl DA relative to DA (65, 66). There is evidence suggesting that the neurons containing greater amounts of neuromelanin, a polymerization product of oxidized DA, are most susceptible to neuronal death in PD (67, 68). The possibility of DA oxidation-induced apoptosis in PD brain has not been evaluated. However, apoptotic cell death has been identified in the hippocampus from postmortem Alzheimer's brain, and apoptotic cells are co-localized with c-Jun proteins, suggesting a poten-

tial mechanism for neurodegenerative disease (69, 70).

Like other *in vitro* studies, DA produces apoptosis in a concentration range between 0.1 and 0.5 mM. This concentration is much higher than that needed for physiological function in the synapse (low micromolar levels) (71). However, we believe that our observations are of potential relevance to pathological situations for the following reasons. 1) We exposed the cells to DA during a relatively short 30-h period and observed apoptosis and its associated biochemical signaling, while the neurodegeneration process *in vivo* may develop over decades. 2) We carried out experiments with healthy young cells possessing a strong anti-oxidative stress system. In the aged individual developing Parkinsonism, there occurs a deteriorating metabolic system with reduced defense ability against ROS produced by DA oxidation. We are currently investigating these problems in rats with different age groups.

In summary, we have presented data to show that DA can induce apoptosis in both dividing cells and neonatal striatal neuronal cell cultures. The DA-induced apoptosis occurs in a time- and concentration-dependent manner. Corresponding to its apoptotic action, DA activates the JNK pathway indicated by stimulation of JNK, phosphorylation of c-Jun, and increase of c-Jun and occurs before activation of a cell "suicide" program. A negative mutant SEK1(Lys → Arg) blocks DA-induced JNK activation and subsequent apoptosis. The c-Jun negative mutant also prevents DA-induced apoptosis. Anti-oxidants including both NAC and catalase can block both DA-induced JNK activation and apoptosis, indicating that DA-induced oxidative stress is involved. Since the anti-oxidation defense system declines during aging, DA-induced apoptosis with involvement of the JNK pathway may play a role in neuron loss from the striatum during aging and Parkinson's and Huntington's diseases, age-related dopaminergic neurodegenerative disease. The demonstration of the oxidation-JNK pathway in DA-induced apoptosis may offer potential means to protect against the damage of aging and age-related diseases, such as increasing defenses against free radicals and blocking the JNK activation pathway.

Acknowledgments—We thank Drs. Y. Liu and Y. Wang for helpful discussions; Dr. N. J. Holbrook for critical reading of the manuscript and constructive suggestions; Dr. L. Zon and J. Kyriakis for SEK1(Lys → Arg) vector; Dr. L. Rubin and J. Ham for pCDFLAGΔ169 DNA.

REFERENCES

- Buisson, A., Callebaut, J., Mathieu, E., Plotkine, M., and Boulu, R. (1992) *J. Neurochem.* **59**, 1153–1157.
- Filloux, F., and Wamsley, J. (1991) *Synapse* **8**, 281–288.
- Schmidt, C., Ritter, J., Sonsalla, P., Hanson, G., and Gibb, J. (1985) *J. Pharmacol. Exp. Ther.* **233**, 539–544.
- O'Dell, S., Weismuller, F., and Marshall, J. (1991) *Brain Res.* **564**, 256–260.
- Akiyama, Y., Koshimura, K., Ohue, T., Lee, K., Miwa, S., Yamagata, S., and Kikuchi, H. (1991) *J. Neurochem.* **57**, 997–1002.
- Hastings, T., Lewis, D., and Zigmond, M. (1996) *Proc. Natl. Acad. Sci. U. S. A.* **93**, 1956–1961.
- Zilkha-Falb, R., Ziv, I., Nardi, N., Offen, D., Melamed, E., and Barzilai, A. (1997) *Cell Mol. Neurobiol.* **17**, 101–118.
- Ziv, I., Melamed, E., Nardi, N., Luria, D., Achiron, A., Offen, D., and Barzilai, A. (1994) *Neurosci. Lett.* **170**, 136–140.
- Michel, P., and Hefti, F. (1990) *J. Neurosci. Res.* **28**, 428–431.
- Hastings, T. G. (1995) *J. Neurochem.* **64**, 919–924.
- Graham, D. (1978) *Mol. Pharmacol.* **14**, 633–643.
- Cohen, G., and Heikkilä, R. E. (1974) *J. Biol. Chem.* **249**, 2447–2452.
- Jellinger, K., Kienzl, E., Rumpelmaier, G., Riederer, P., Stachelberger, H., Ben-Shachar, D., and Youdim, M. B. (1992) *J. Neurochem.* **59**, 1168–1171.
- Halliwel, B. (1992) *J. Neurochem.* **59**, 1609–1623.
- Adams, J. D. J., and N. O. I. (1991) *Free Radical Biol. Med.* **10**, 161–169.
- Olanow, C. W., and Arendash, G. W. (1994) *Curr. Opin. Neurol.* **7**, 548–558.
- Hirsch, E. C., Brandel, J.-P., Galle, P., Javoy-Agid, F., and Agid, Y. (1991) *J. Neurochem.* **56**, 446–451.
- Jenner, P. (1993) *Acta Neurol. Scand. Suppl.* **146**, 6–13.
- Shinkai, T., Zhang, L., Mathias, S., and Roth, G. (1997) *J. Neurosci. Res.* **47**, 393–399.
- Cheng, N.-N., Maeda, T., Kume, T., Kaneko, S., Kochiyama, H., Akaike, A., Goshima, Y., and Misu, Y. (1996) *Brain Res.* **743**, 278–283.
- Masserano, J., Gong, L., Kulaga, H., Baker, I., and Wyatt, R. (1996) *Mol. Pharmacol.* **50**, 1309–1315.
- Simantov, R., Blinder, E., Ratovitski, T., Tauber, M., Gabbay, M., and Porat, S. (1996) *Neuroscience* **74**, 39–50.
- Walkinshaw, G., and Waters, C. (1994) *Neuroscience* **63**, 975–987.
- Offen, D., Ziv, I., Gorodin, S., Barzilai, A., Malik, A., and Melamed, E. (1995) *Biochim. Biophys. Acta* **1268**, 171–177.
- Chen, Y.-R., Wang, X., Templeton, D., Davis, R., and Tan, T.-H. (1996) *J. Biol. Chem.* **271**, 31929–31936.
- Dérjard, B., Raingeaud, J., Barrett, T., Wu, I.-H., Han, J., Ulevitch, R., and Davis, R. (1995) *Science* **267**, 682–685.
- Dérjard, B., Hibi, M., Wu, I.-H., Barrett, T., Su, B., Deng, T., Karin, M., and Davis, R. (1994) *Cell* **76**, 1025–1037.
- Kyriakis, J., Banerjee, P., Nikolakaki, E., Dai, T., Rubie, E., Ahmad, M., Avruch, J., and Woodgett, J. (1994) *Nature* **369**, 596–600.
- Verheij, M., Bose, R., Lin, X., Yao, B., Jarvis, W., Grant, S., Birrer, M., Szabo, E., Zon, L., Kyriakis, J., Haimovitz-Friedman, A., Fuks, Z., and Kolesnick, R. (1996) *Nature* **380**, 75–79.
- Xia, Z., Dickens, M., Raingeaud, J., Davis, R., and Greenberg, M. (1995) *Science* **270**, 1326–1331.
- Ichijo, H., Nishida, E., Irie, K., Dijke, P., Saitoh, M., Moriguchi, T., Takagi, M., Matsumoto, K., Miyazono, K., and Gotoh, Y. (1997) *Science* **275**, 90–94.
- Ham, J., Bahij, C., Whitfield, J., Pfarr, C., Lallemand, D., Yaniv, M., and Rubin, L. (1995) *Neuron* **14**, 927–939.
- Mesrobian, E., Joseph, J., and Roth, G. (1992) *J. Neurosci. Res.* **31**, 341–345.
- Coso, O. A., Chiariello, M., Kalinec, G., Kyriakis, J., Woodgett, J., and Gutkind, J. S. (1995) *J. Biol. Chem.* **270**, 5620–5624.
- Wyllie, A. (1980) *Nature* **284**, 555–556.
- Gyros, B., Sokoloff, P., Martres, M.-P., Riou, J.-F., Emorine, L., and Schwartz, J.-C. (1989) *Nature* **342**, 923–926.
- Valerio, A., Alberici, A., Tinti, C., Spano, P., and Memo, M. (1994) *J. Neurochem.* **62**, 1260–1266.
- Chen, Y.-R., Meyer, C. F., and Tan, T.-H. (1996) *J. Biol. Chem.* **271**, 631–634.
- Brown, P., Chen, T., and Birrer, M. (1994) *Oncogene* **9**, 791–799.
- Hirai, S., Ryseck, R., Mehta, F., Bravo, R., and Yaniv, M. (1989) *EMBO J.* **8**, 1433–1439.
- Estus, S., Zaks, W., Freeman, R., Gruda, M., Bravo, R., and Johnson, E. J. (1994) *J. Cell Biol.* **127**, 1717–1727.
- Schlingensiepen, K., Schlingensiepen, R., Kunst, M., Klinger, I., Gerdes, W., Seifert, W., and Brysch, W. (1993) *Dev. Genet.* **14**, 305–312.
- Liu, Y., Gorospe, M., Yang, C., and Holbrook, N. J. (1995) *J. Biol. Chem.* **270**, 8377–8380.
- Davis, R. (1994) *Trends Biochem. Sci.* **19**, 470–473.
- Rubin, L., Philpott, K., and Brooks, S. (1993) *Curr. Biol.* **3**, 391–394.
- Rubin, L., Gatchalian, C., Rimon, G., and Brooks, S. (1994) *Curr. Opin. Neurobiol.* **4**, 696–702.
- Freeman, R., Estus, S., and Johnson, E. (1994) *Neuron* **12**, 343–355.
- Yan, C. Y. I., Ferrari, G., and Greene, L. A. (1995) *J. Biol. Chem.* **270**, 26827–26832.
- Hockenbery, D., Oltvai, Z., Yin, X.-M., Millman, C., and Korsmeyer, S. (1993) *Cell* **75**, 241–251.
- Park, D. S., Stefanis, L., Yan, C. Y. I., Farinelli, S. E., and Greene, L. A. (1996) *J. Biol. Chem.* **271**, 21898–21905.
- Abad, F., Maroto, R., López, M., Sánchez-García, P., and García, A. (1995) *Eur. J. Pharmacol.* **293**, 55–64.
- Roth, G., and Joseph, J. (1994) *Ann. N. Y. Acad. Sci.* **719**, 129–135.
- Lai, H., Bowden, D., and Horita, A. (1987) *Neurobiol. Aging* **8**, 45–49.
- Han, Z., Kuyatt, B., Kochman, K., DeSouza, E., and Roth, G. (1989) *Brain Res.* **298**, 299–307.
- Zhang, L., Kokkonen, G., and Roth, G. (1995) *Brain Res.* **677**, 177–179.
- Benzi, G., Pastoris, O., Marzatico, F., Villa, R., Dagani, F., and Curti, D. (1992) *Neurobiol. Aging* **13**, 361–368.
- Bossi, S., Simpson, J., and Isacson, O. (1993) *Neuroreport* **4**, 73–76.
- Smith, C., Carney, J., Starke-Reed, P., Oliver, C., Stadtman, E., Floyd, R., and Markesbery, W. (1991) *Proc. Natl. Acad. Sci. U. S. A.* **88**, 10540–10543.
- Oppenheim, R. (1991) *Annu. Rev. Neurosci.* **14**, 453–501.
- Bursch, W., Oberhammer, F., and Schulte-Hermann, R. (1992) *Trends Pharmacol. Sci.* **13**, 245–251.
- Todd, R. D. (1992) *Biol. Psychiatry* **31**, 794–807.
- Drukarch, B., Jongenelen, C. A., Schepens, E., Langeveld, C. H., and Stoof, J. C. (1996) *J. Neurosci.* **16**, 6038–6045.
- Berman, S. B., Zigmond, M. J., and Hastings, T. G. (1996) *J. Neurochem.* **67**, 593–600.
- Jonsson, G. (1971) *Prog. Histochem. Cytochem.* **2**, 299–344.
- Fornstedt, B., Brun, A., Rosengren, E., and Carlsson, A. (1989) *J. Neural Transm. Park. Dis. Dement. Sect. 1*, 279–295.
- Fornstedt, B., and Carlsson, A. (1989) *J. Neural Transm.* **76**, 155–161.
- Kastner, A., Hirsch, E. C., Herrero, M. T., Javoy-Agid, F., and Agid, Y. (1993) *J. Neurochem.* **61**, 1024–1034.
- Hirsch, E., Graybiel, A., and Agid, Y. (1988) *Nature* **334**, 345–348.
- Su, J. H., Anderson, A. J., Cummings, B. J., and Cotman, C. W. (1994) *Neuroreport* **5**, 2529–2533.
- Anderson, A. J., Su, J. H., and Cotman, C. W. (1996) *J. Neurosci.* **16**, 1710–1719.
- Madison, D. V., and Nicoll, R. A. (1982) *Nature* **299**, 636–638.